J. Electroanal. Chem., 331 (1992) 913–924
Elsevier Sequoia S.A., Lausanne
JEC 05017

Application of rapid scan cyclic voltammetry to a study of the oxidation and dimerization of *N,N*-dimethylaniline in acetonitrile *

Hongjun Yang, David O. Wipf and Allen J. Bard

Department of Chemistry and Biochemistry, The University of Texas at Austin, Austin, TX 78712 (USA)

(Received 28 October 1991; in revised form 10 December 1991)

Abstract

Rapid scan cyclic voltammetry was used to investigate the mechanism of the anodic oxidation and dimerization of *N,N*-dimethylaniline (DMA) in acetonitrile solution. The reduction wave for the $DMA^{\cdot+}$ radical cation was observed at scan rates above 500 V s^{-1}. Electrogenerated $DMA^{\cdot+}$ radical cations underwent a second-order radical cation–radical cation coupling with deprotonation to form *N,N,N',N'*-tetramethylbenzidine; no evidence of polymerization was detected. The experimental results best fit an EC_2EE reaction mechanism determined by fitting the data with working curves obtained by digital simulation. A rate constant of 6.3×10^5 M^{-1} s^{-1} was found for the coupling reaction. The clean reaction process suggests that the oxidation of DMA can serve as a model for the EC_2EE reaction mechanism in kinetic studies.

INTRODUCTION

We report here a study of the mechanism of the anodic oxidation of *N,N*-dimethylaniline in acetonitrile using rapid scan cyclic voltammetry. The oxidation of aniline in aqueous and non-aqueous solutions results in the formation of a conducting polyaniline film, and many investigations of the anodic behavior of aniline and the electrochemical, electrical and physicochemical properties of polyaniline have appeared [1–13]. New types of polymer films formed electrochemically from *N,N*-dialkylaniline derivatives have also attracted considerable attention [14–18], because the electropolymerization of these derivatives leads to "ionene polymers" with quaternary ammonium sites in the polymeric backbone.

* Dedicated to Professor Roger Parsons on the occasion of his retirement from the University of Southampton and in recognition of his contributions to electrochemistry.

These have an anion exchange character over a wide range of pH and can be used for the modification of electrode surfaces.

Early studies, e.g. by Adams and coworkers [19–25], showed that the anodic oxidation of aniline and its derivatives in aqueous and non-aqueous solutions usually occurs via a number of reactions and leads to a large number of products, depending upon the reaction conditions. The number of reaction pathways diminished considerably when the amine N atoms were substituted with alkyl groups. However, even for *N,N*-dialkylanilines, Hand and Nelson reported [26,27] that the reaction pathways were still diverse and depended strongly on the concentration of amine and the time of electrolysis. On the other hand, the lifetime of the primary radical cation of *N,N*-dialkylaniline is not greatly affected by the alkyl group and no reduction wave for the initially generated radical cation was observed in previous studies [19–27]. Thus it has been difficult to resolve the detailed mechanism of the anodic oxidation of these substituted anilines.

Recently we reported the mechanism of diphenylamine oxidation, radical cation dimerization and polymerization in acetonitrile [28]. Here we investigate the oxidation pathways of *N,N*-dimethylaniline in acetonitrile solution at an ultramicroelectrode (UME) by fast scan cyclic voltammetry and propose a mechanism for the oxidation reaction.

EXPERIMENTAL

The electrochemical cell and measurement procedures have been described previously [28]. Potentials were measured vs. a silver quasi-reference electrode (AgQRE) whose potential was calibrated against the decamethylferrocene/decamethylferrocinium couple ($E_{1/2} = -0.12$ V vs. the saturated calomel electrode (SCE)) [29]. All potentials are reported vs. the SCE.

N,N-dimethylaniline (DMA, 99%, Aldrich Chemical Company, Milwaukee, WI) was used as received. *N,N,N',N'*-tetramethylbenzidine (TMB, Eastman Kodak, Rochester, NY) was recrystallized from methanol. Tetrabutylammonium hexafluorophosphate ($TBAPF_6$, Southwestern Analytical Chemicals, Austin, TX), the supporting electrolyte, was recrystallized twice from ethanol and acetone. Acetonitrile (MeCN, 0.004% water, Burdick & Jackson) was used as received, but about 0.5 g ICN Alumina N-Super 1 (ICN Biomedicals, Costa Mesa, CA) was added to the solution of MeCN + $TBAPF_6$ for further drying. Other chemicals were reagent grade and were used as received.

Before the addition of DMA to the MeCN with supporting electrolyte, the solution was purged with argon for about 10 min until the background voltammogram (checked by potential sweeps between 2.0 and −2.0 V) was flat. The solution was kept in an argon atmosphere during the entire experiment.

When scan rates above 10 kV s^{-1} were used, a two-electrode (platinum UME and AgQRE) cell configuration was employed to avoid the distortion at fast scan rates from a three-electrode configuration. A two-electrode home-built potentio-

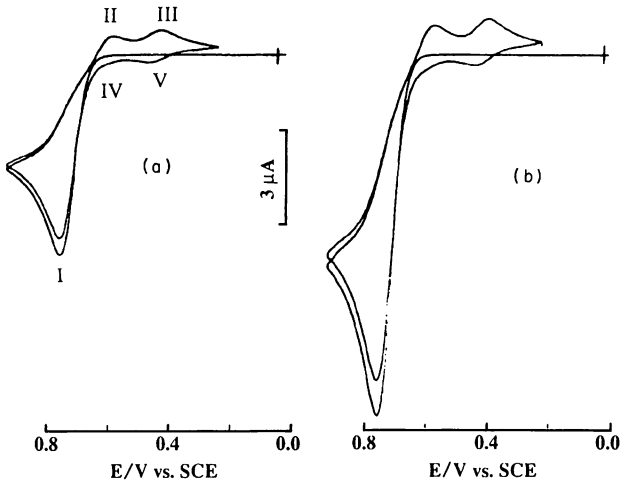

Fig. 1. Cyclic voltammograms of 6.31 mM *N,N*-dimethylaniline in acetonitrile containing 0.1 M $TBAPF_6$ with 0.5 mm platinum disk, 0.1 V s^{-1}, (a) in the absence and (b) in the presence of pyridine.

stat based on previous designs [30] was used. The current-to-voltage converter of this instrument has a time constant of 100 ns. A function generator (Model 2400, Krohn-Hite Corporation, Avon, MA) served as the waveform generator. A Tektronix 2440 digital storage oscilloscope (500 megasamples per second, Tektronix, Beaverton, OR) was used for data acquisition and display. Data were transferred to an IBM personal computer for storage and processing.

RESULTS AND DISCUSSION

Cyclic voltammograms of DMA in MeCN solution

As shown in previous studies [20–22], the cyclic voltammogram of DMA obtained at a platinum disk electrode in MeCN–0.1 M $TBAPF_6$ at a low scan rate ($v = 100$ mV s^{-1}) shows only one peak on the first positive scan at a potential of about 0.76 V (SCE) with no reversal peak in the negative scan (Fig. 1a). The single irreversible anodic peak was present on the initial scan at values of v up to 500 V s^{-1}, indicating that the product, $DMA^{\cdot+}$, is unstable at these time scales. Several new peaks were observed in the negative scan and the second positive scan. Peaks II, IV and III, V represent two new redox couples. Peak IV is merged with peak I, but as the scan rate was increased, peak IV separated into a distinct wave. The peak potential separations ΔE_p for II–IV and III–V were both about 60 mV, consistent with a reversible electron transfer. Upon repeated scans, the current–

potential curve reached a steady state with no indication of the formation of a polymer film.

According to earlier studies [20–22], the major product from DMA oxidation in aqueous and non-aqueous solutions was the *p–p* (C–C) coupled compound *N,N,N′,N′*-tetramethylbenzidine (TMB). TMB is more easily oxidized than DMA and forms a stable dication. However, some isomeric benzidines such as *o–o*-TMB and *o–p*-TMB were also thought to be present [26]. For the experiments described here, other possible coupling products such as 4,4′-methylenebis (*N,N*-dimethylaniline) and crystal violet are not considered; because of the low concentration of starting material and short electrolysis time, their formation is unlikely [26]. An outline of the reaction scheme for the electro-oxidation of DMA is as follows:

$$DMA - e^- \rightleftharpoons DMA^{\cdot+} \quad (1)$$

$$2DMA^{\cdot+} \rightarrow TMB + 2H^+ \quad (2)$$

$$TMB - e^- \rightleftharpoons TMB^+ \quad (3)$$

$$TMB^+ - e^- \rightleftharpoons TMB^{2+} \quad (4)$$

We examined the details of this mechanism (1) to provide proof of the existence of the $DMA^{\cdot+}$ radical cation, (2) to study the effect of solution acidity on the coupling reaction and (3) to distinguish radical ion–radical ion coupling or radical ion–parent coupling [28].

Identification of the dimerization product as TMB

As we have mentioned, some uncertainty exists in the way coupling, e.g. C–C, C–N and N–N, proceeds to form different dimer products. Under conditions of neutral MeCN solution, low concentrations of DMA and a short electrolysis time scale, C–N and N–N couplings can be ruled out [27]. Figure 2a shows the cyclic voltammogram (CV) of an authentic sample of TMB. Two reversible redox waves appear in both positive and negative scans. Figures 2b–2d show that the voltammograms are the same for DMA added to the TMB solution or vice versa. The peak potentials in Fig. 2a are identical to those in Figs. 2b–2d. While cyclic voltammograms are not a strictly reliable tool for the identification of the electrochemically generated products, these results complement the spectroscopic results reported by Mizoguchi and Adams [20], who reported only the presence of the *p–p* isomer. Thus the radical cations of $DMA^{\cdot+}$ undergo a *p–p* C–C coupling and TMB is the only dimerization product under our experimental conditions. Further coupling reactions to form polymers, as seen for aniline and diphenylamine, also do not occur.

Effect of solution acidity

Note that the radical cation coupling reaction in eqn. (2) is associated with deprotonation. DMA itself is a moderate base, so it can serve as a proton acceptor. The protonated DMA, $DMAH^+$, is electroinactive. Progressive addition of perchloric acid to a solution containing 3.9 mM DMA and 0.1 M $TBAPF_6$ in MeCN caused a decrease and finally the disappearance of the DMA oxidation wave and

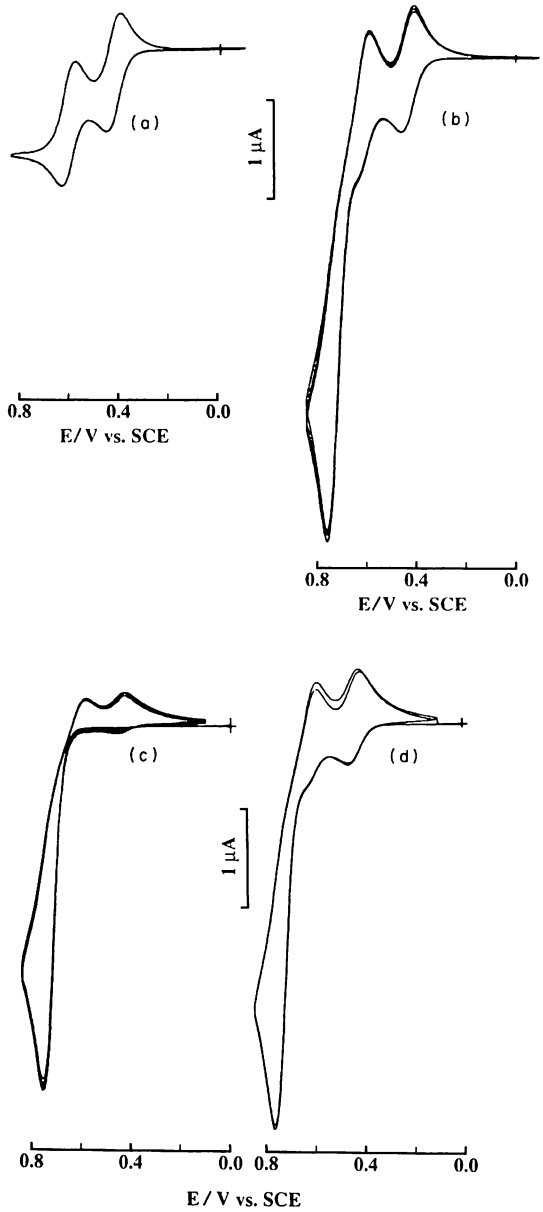

Fig. 2. Cyclic voltammograms of (a) 0.79 mM TMB alone, (b) 3.15 mM DMA added to (a), (c) 3.15 mM DMA alone and (d) 0.54 mM TMB added to (c). Other conditions were the same as in Fig. 1.

associated reversal waves. With DMA acting as a base, reaction (2) should be rewritten as

$$2DMA^{\cdot+} + 2DMA \rightarrow TMB + 2DMAH^{+} \quad (5)$$

In this case the overall reaction, summing reactions (1), (5), (3) and (4), is

$$4DMA - 4e^- \rightarrow TMB^{2+} + 2DMAH^+ \quad (6a)$$

and one electron is lost per DMA molecule, i.e. $n_{app} = 1$. When the mechanism of the reaction is probed by investigating the effects of bulk concentration c^* and scan rate v on the height of peak I in the first scan, an $n_{app} = 1$ would make this mode of diagnosis much less applicable. In contrast, summing eqns. (1)–(4) leads to the overall reaction

$$2DMA - 4e^- \rightarrow TMB^{2+} + 2H^+ \quad (6b)$$

which implies that in the presence of a stronger base than DMA, $n_{app} = 2$. In this case one can examine the extent of occurrence of reaction (2) during the scan (i.e. considering the dimensionless parameter $kc^*/v(RT/F)$, where k is the rate constant of reaction (2)). When this parameter is small, $n_{app} \rightarrow 1$; when it is large, $n_{app} \rightarrow 2$, assuming no DMA protonation, because oxidation of TMB to TMB^{2+} (reactions (3) and (4)) occurs at the potential of the first anodic wave. Thus, if x is the fraction of $DMA^{\cdot+}$ converted to TMB during the scan, the overall reaction in that time period is

$$DMA - (1+x)\,e^- \rightarrow (x/2)TMB^{2+} + (1-x)DMA^{\cdot+} + H^+ \quad (7)$$

and $n_{app} = 1 + x$. However, if the free protons in reaction (7) are scavenged by monomer DMA, the overall reaction becomes

$$(1+x)DMA - (1+x)\,e^- \rightarrow (x/2)TMB^{2+} + (1-x)DMA^{\cdot+} + xDMAH^+ \quad (8)$$

In this case $n_{app} = 1$, independently of x. Therefore n_{app} will be a constant, no matter how the parameter $kc^*/v(RT/F)$ varies. Clearly the intervention of protonation reactions of DMA complicates the interpretation of the CV behavior in terms of reaction mechanism. Thus finding a proper proton scavenger is the key to further investigation.

In our previous study of the diphenylamine system [28], because diphenylamine is a weak base, a small amount of water added to the dry MeCN solution played the role of proton acceptor. However, DMA is a stronger base and water added to the solution does not change the electrochemical behavior of DMA at these time scales. Therefore, with DMA, pyridine was used as a proton scavenger. As pyridine was added to the DMA solution, the current for peak I increased and its width decreased; the positions of all the peaks did not change. When the concentration of pyridine in the solution was equal to that of DMA, the current of peak I reached a maximum value of twice that obtained without addition of the pyridine solution (Fig. 1b), suggesting a two-electron process. Under these conditions the overall reaction is now

$$2DMA + 2Py - 4e^- \rightarrow TMB^{2+} + 2PyH^+ \quad (9)$$

Thus the presence of pyridine (at about the same concentration as DMA) simplifies the CV study and allows the observation of a variation in n_{app} between 1 and 2 as a function of c^* and v to probe the reaction mechanism.

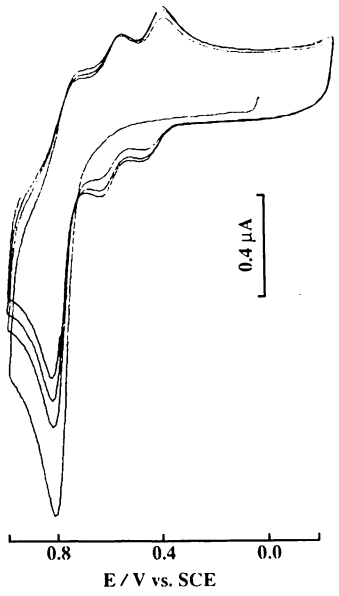

Fig. 3. Cyclic voltammogram of 3.94 mM DMA in 0.1 M $TBAPF_6$ + acetonitrile with 25 μm diameter platinum microelectrode at 500 V s^{-1}.

Radical cation–radical cation coupling vs. radical cation–parent coupling in the dimerization reaction

For an oxidative coupling reaction it is difficult to distinguish a mechanism with radical cation–radical cation coupling from radical cation–parent coupling. The possibility of disproportionation should also be considered. Our previous paper [28] discussed these problems in detail and presented three diagnostic criteria to distinguish among the mechanisms. Here these criteria were used with an examination of the change in the normalized peak current in the first wave and the shape of the CV wave as a function of scan rate and concentration. The measurements were carried out with ultramicrodisk electrodes, so that fast scan rates could be used to bring the characteristic time window into a region where kinetic effects would be revealed. To show the full range of variation of n_{app} from 2 to 1, the scan rate was varied over a range of about six orders of magnitude.

At a scan rate of 500 V s^{-1} (Fig. 3) a small reduction wave of $DMA^{\cdot+}$ is observed on scan reversal while the two one-electron transfer waves of the dimer TMB still remain, indicating that the chemical coupling is fast. However, at higher scan rates (Fig. 4) the TMB waves disappear and only the wave for the DMA–$DMA^{\cdot+}$ remains. Although the CV wave is distorted by charging current and some uncompensated ohmic drop, the waves show a chemically reversible system. This is

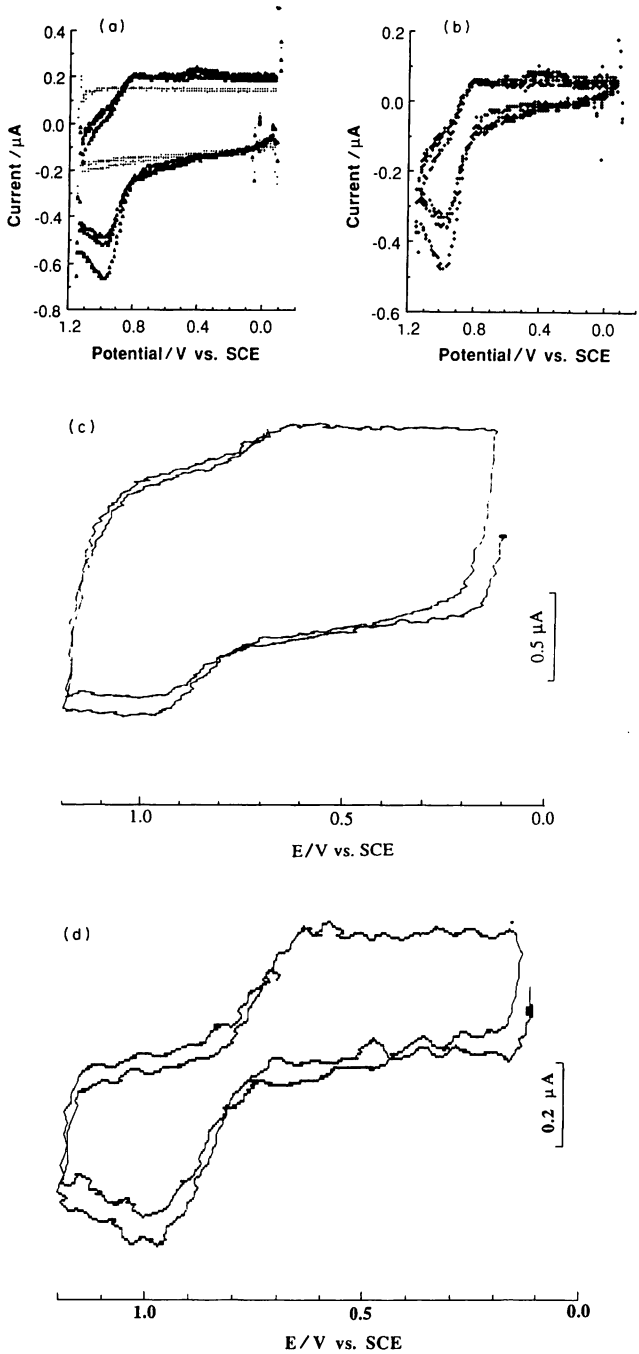

Fig. 4. Cyclic voltammograms of 3.94 mM DMA in the presence of pyridine (a) at 10 μm diameter platinum microelectrode, $\upsilon = 8000$ V s^{-1}; (b) as in (a) but with subtraction of background; (c) at 5 μm diameter platinum microelectrode, $\upsilon = 10^5$ V s^{-1}; (d) as in (c) but with subtraction of background and Fourier filtering to remove high frequency noise.

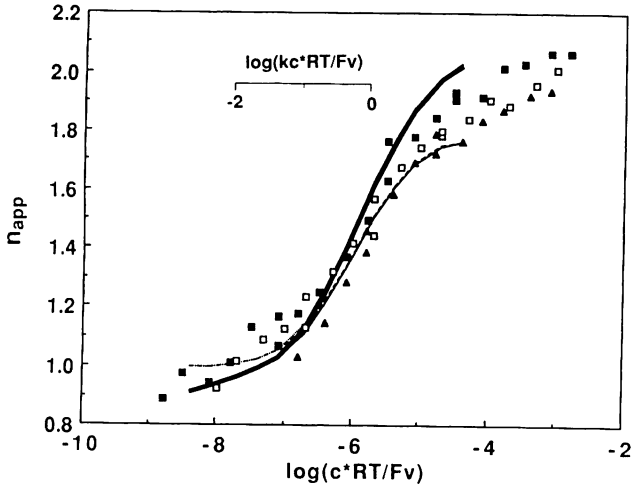

Fig. 5. Normalized current of the first peak vs. $\log(c^*RT/Fv)$. DMA concentrations: (▲) 3.15 mM, (□) 3.94 mM, (■) 6.31 mM with presence of pyridine. Lines are simulated working curves for different proposed mechanisms: (——) R–R coupling, $k^\circ = 1.0$ cm s^{-1}, (· · · · · ·) $k^\circ = 10^{10}$ cm s^{-1}; (———) R–P coupling, $k^\circ = 1.0$ cm s^{-1}, (— — —) $k^\circ = 10^{10}$ cm s^{-1}.

strong evidence for the existence of the stable radical cation $DMA^{\cdot+}$ at this time scale ($\tau \approx RT/Fv \approx 0.25$ μs).

To normalize the peak current of the first wave, the diffusion coefficient of DMA was measured by chronoamperometry in the absence of pyridine at microdisk electrodes and by the variation in steady-state current vs. radii of microdisk electrodes in the presence of pyridine. The first method does not require knowledge of the bulk concentration or the number of electrons participating in the electrode reaction [31]. The results of these two methods were 2.24×10^{-5} and 2.41×10^{-5} cm^2 s^{-1} respectively. Experimental data for the normalized peak current at various scan rates and concentrations are shown in Fig. 5. The simulated working curves are overlaid on the experimental data. We have used the abbreviation R–R to denote a radical cation–radical cation coupling pathway and R–P to denote a radical cation–parent coupling. Given the scatter in the experimental data, it is difficult to distinguish between the R–P and R–R coupling mechanisms. A rate constant of 6.3×10^5 M^{-1} s^{-1} is obtained from the R–R mechanism fit to the data. A working curve for the disproportionation reaction is not shown because all those curves were located below the R–P curve. The R–R mechanism was favored from a consideration of the shape of the first wave. We have shown that the potential difference between the peak and the half-peak is a useful way to distinguish between the dimerization coupling routes [28]. These results are shown in Fig. 6 and again favor the R–R route at slow scan rates. The deviations at fast scan rates are mainly due to the uncompensated resistance and perhaps the onset of heterogeneous kinetic effects.

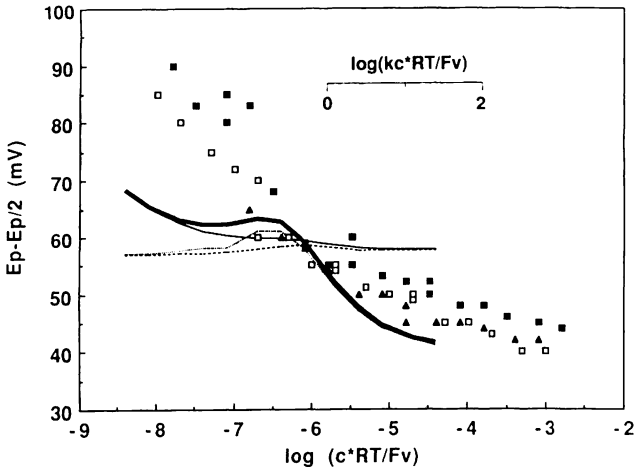

Fig. 6. Variation in $E_p - E_{p/2}$ vs. $\log(c^*RT/Fv)$. DMA concentrations: (▲) 3.15 mM, (□) 3.94 mM, (■) 6.31 mM with presence of pyridine. Lines are simulated working curves for different proposed mechanisms: (——) R–R coupling, $k^o = 1.0$ cm s^{-1}, (·····) $k^o = 10^{10}$ cm s^{-1} (———) R–P coupling, $k^o = 1.0$; cm s^{-1}, (— — —) $k^o = 10^{10}$ cm s^{-1}.

Many aspects of the EC_2EE type of reaction mechanism for anodic oxidation and dimerization of DMA have been revealed. The question as to the stage of the reaction at which deprotonation occurs still remains. According to the literature, deprotonation is usually extremely fast (i.e. about 10^7 s^{-1}) [32]. If deprotonation of the radical cation occurs first and is followed by R–R coupling ($DMA^{\cdot}$) in the rate-determining step, the overall reaction would also follow the R–R mechanism. This is unlikely in our case and we believe deprotonation occurs after radical cation coupling, because if it occurred prior to the coupling, the reversal wave of $DMA^{\cdot+}$ would not be detected at scan rates of 500 V s^{-1} and higher. After we concluded this work, a brief communication on the anodic oxidation of several tertiary amines appeared [33], in which DMA was also studied by cyclic voltammetry with ultramicroelectrodes. The authors also concluded that the reaction occurs by the R–R route (or DIM1 route) by a consideration of the shift in E_{pa} with v and estimated the rate constant of R–R coupling for $DMA^{\cdot+}$ as 1.5×10^7 M^{-1} s^{-1} by comparison of the shapes of the voltammetric curves with the simulated curves.

CONCLUSIONS

Cyclic voltammetry with ultramicroelectrodes is an effective technique for studying the mechanism of the initial stage of anodic oxidation and dimerization of *N*,*N*-dimethylaniline in acetonitrile. The presence of pyridine as a proton acceptor simplifies the interpretation of the voltammetry. Under these conditions the net faradaic charge passed during the electrode reaction is two electrons per DMA

monomer. The $DMA^{\cdot+}$ undergoes a second-order radical cation–radical cation coupling to form *N,N,N′,N′*-tetramethylbenzidine (TMB), which is further oxidized through two one-electron transfer steps to TMB^{2+}. A chemically reversible wave for the reduction of the radical cation $DMA^{\cdot+}$ was observed at scan rates higher than 500 V s^{-1} and a rate constant for the coupling reaction is 6.3×10^5 M^{-1} s^{-1}.

Since no further polymerization occurs and the dimerization product TMB is soluble in acetonitrile, the anodic oxidation and dimerization of DMA is a good model for the EC_2EE reaction.

ACKNOWLEDGMENT

The support of this research by the National Science Foundation (NSF CHE8901450) is gratefully acknowledged.

REFERENCES

1 A.F. Diaz and J. Bargon, in T.A. Skotheim (Ed.), Handbook of Conducting Polymers, Vol. 1, Marcel Dekker, New York, 1986, pp. 81–116.
2 E.M. Genies, A. Boyle, M. Lapkowski and C. Tsintavis, Synth. Met., 36 (1990) 182.
3 A.G. McDiarmid, J.C. Chiang, A.F. Richter, N.L.D. Somasiri and A.J. Epstein, in L. Alcacer (Ed.), Conducting Polymers, Special Applications, Reidel, Dordrecht, 1987, p. 105.
4 A.F. Diaz and J.A. Logan, J. Electroanal. Chem., 111 (1980) 111.
5 W.-S. Huang, B.D. Humphrey and A.G. McDiarmid, J. Chem. Soc., Faraday Trans. 1, 82 (1986) 2385.
6 A. Kitani, M. Kaya and K. Sasaki, J. Electrochem. Soc., 133 (1986) 1069.
7 A.G. McDiarmid, S.L. Mu, N.L. Somasiri and W. Wu, Mol. Cryst. Liq. Cryst., 121 (1985) 187.
8 G. Mengoli, M.T. Munari, P. Biacco and M.M. Musiani, J. Appl. Polym. Sci., 26 (1981) 4247.
9 R. Noufi, A.J. Nozik, J. White and L.F. Warren, J. Electrochem. Soc., 129 (1982) 2261.
10 G. Mengoli, M.M. Musiani, G. Zotti and S. Valcher, J. Electroanal. Chem., 202 (1986) 217.
11 K. Hyodo and M. Omae, J. Electroanal. Chem., 292 (1990) 93.
12 T. Kobayashi, H. Yoneyama and H. Tamura, J. Electroanal. Chem., 161 (1984) 419.
13 E.W. Paul, A.J. Ricco and M.S. Wrighton, J. Phys. Chem., 89 (1985) 1441.
14 N. Oyama, T. Ohsaka and T. Shimizu, Anal. Chem., 57 (1985) 1526.
15 T. Ohsaka, T. Okajima and N. Oyama, J. Electroanal. Chem., 200 (1986) 159.
16 T. Ohsaka, T. Okajima and N. Oyama, J. Electroanal. Chem., 215 (1986) 191.
17 T. Ohsaka, K. Taguchi, S. Ikeda and N. Oyama, Denki Kagaku, 58 (1990) 1136.
18 J. Yano, J. Electrochem. Soc., 138 (1991) 455.
19 R.N. Adams, Electrochemistry at Solid Electrodes, Marcel Dekker, New York, 1969.
20 T. Mizoguchi and R.N. Adams, J. Am. Chem. Soc., 84 (1962) 2058.
21 Z. Galus and R.N. Adams, J. Am. Chem. Soc., 84 (1962) 2061.
22 Z. Galus, R.M. White, F.S. Rowland and R.N. Adams, J. Am. Chem. Soc. 84 (1962) 2065.
23 Z. Galus and R.N. Adams, J. Phys. Chem., 67 (1963) 862.
24 E.T. Seo, R.F. Nelson, J.M. Fritsch, L.S. Marcoux, D.W. Leedy and R.N. Adams, J. Am. Chem. Soc., 88 (1966) 3498.
25 N.L. Weinberg and T.B. Reddy, J. Am. Chem. Soc., 90 (1968) 91.
26 R. Hand and R.F. Nelson, J. Electrochem. Soc., 117 (1970) 1353.
27 R.F. Nelson, in A. Weissberger (Ed.), Techniques of Chemistry, Vol. 5; N.L. Weinberg (Ed.), Technique of Electroorganic Synthesis, Part 1, Wiley, New York, 1974, pp. 591–779.
28 H. Yang and A.J. Bard, J. Electroanal. Chem., 306 (1991) 87.

29 C. Zou and M.S. Wrighton, J. Am. Chem. Soc., 112 (1990) 7578.
30 D.O. Wipf, Ph.D. Dissertation, Indiana University, Bloomington, IN, 1989.
31 G. Denuault, M.V. Mirkin and A.J. Bard, J. Electroanal. Chem., 308 (1991) 27.
32 V.D. Parker, G. Sundholm, U. Svanholm, A. Ronlan and O. Hammerich, in A.J. Bard (Ed.), Encyclopedia of Electrochemistry of the Elements, Vol. XI, Marcel Dekker, New York, 1978, pp. 242–269.
33 D. Larumbe, I. Gallardo and C.P. Andieux, J. Electroanal. Chem., 304 (1991) 241.